Toward Stable and Realistic Haptic Interaction for Tooth Preparation Simulation

Jun Wu[a,b], **Dangxiao Wang**[a], **Charlie C. L. Wang**[b], **and Yuru Zhang**[a]
[a] State Key Lab of Virtual Reality Technology and Systems
Beihang University, 100191, Beijing, China (e-mail: wujun@me.buaa.edu.cn)
[b] Department of Mechanical and Automation Engineering
The Chinese University of Hong Kong, Shatin, N.T., Hong Kong, China (e-mail: cwang@mae.cuhk.edu.hk)

Abstract

In this paper, we present the methods to generate a stable and realistic simulator for dental surgery. Firstly, a simplified force model is derived from grinding theory by considering the complex bur shape and dental handpiece's dynamic behavior. While the force model can be evaluated very fast to fulfill the high update rate of haptic rendering, it also explains basic haptic sensation features in tooth preparation operation. Secondly, as direct rendering of this damping-like force model may induce instability of the haptic device, we apply a virtual coupling based method to guarantee the stability in haptic rendering. Furthermore, implicit integration of the bur's motion equation is utilized to ensure numerical stability. Thirdly, to overcome force discontinuity caused by locally removing tooth materials, we define a two-layers based representation for the bur, where the boundary voxels are adopted to compute forces and the interior voxels are employed to remove materials from teeth. The experimental results agree with the real sensation described by experienced dentists.

1 Introduction

Tooth preparation is ubiquitous in dental surgery. This process always involves grinding operation using high-speed rotating burs to modify the shape of the tooth for further treatment. During this operation, too much applied force will increase the rate of heat generation and thus damage the tooth tissues, while too little force may prolong the painful treatment procedure for the patient. Therefore, haptic sensation is very important for the surgeons to operate successfully. How to train students on haptic sensation is problematic. Usually, students in dental training use plastic teeth or removed teeth from patients mounted on a dummy head to practise these operations (as illustrated in Fig. 1). However, it is hard to simulate the stiffness and multi-layered structure of real teeth by plastic ones, and it is difficult to find sufficient number of removed teeth. Therefore, there is a great demand for virtual dental training systems at the dentistry departments of medical schools.

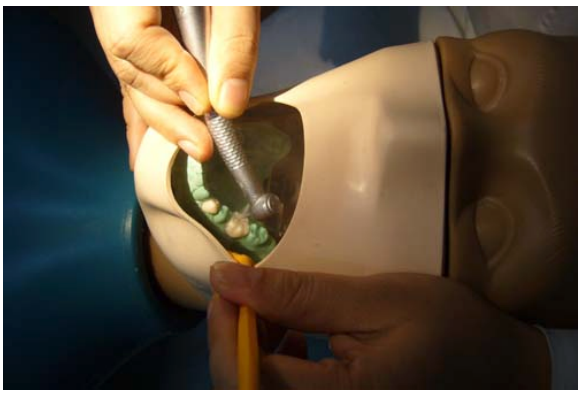

Fig. 1. Dental surgery training in medical schools on real removed teeth on a dummy head.

As simulation techniques provide interactive, safe and reusable patient environment for novices to practise, surgical simulators have shown strong potential in dental education as alternatives to traditional training platforms. Recently, several virtual reality dental training systems incorporating haptic feedback have been developed (e.g., [1, 2, 3, 4, 5]). These systems provide realistic visual, sound and debris simulation, and can record the operations of students for the further evaluation. Besides, other training approach such as haptic playback is also investigated [6]. The effectiveness of virtual training has been proved in initial experiments (ref. [7]).

Nevertheless, few of these dental simulators gives detail description about the fidelity of the feedback force when grinding on teeth. It is believed that unrealistic haptic sensation in training will mislead the dentists in real surgery. The challenge of achieving realism comes from the lack of knowing fundamentals of tooth grinding and the contradictions between fidelity and other requirements in haptic interaction. In short, the fidelity of feedback force, the stability of simulator, and high update rates are generally required. *Fidelity* means that the force feeling during the virtual tooth manipulation is similar to that in real situation. *Stability* refers to the stable running of the haptic device, a mechatronic system.

For a given haptic device, its stability is typically limited by the maximum stiffness of spring force model which can be simulated stably. *High update rates*, specifically the generally agreed $1kHZ$ and $24HZ$ for haptic and graphic rendering loops, are required for continuous force and visual perception (ref. [8]).

Two contradictions exist among these requirements which should be traded off in practice.

(A) *Fidelity and computational efficiency*. To achieve adequate update rates, some simplifications of the grinding-force model and the material removal computation must be adopted, and these will weaken the fidelity of the system in return.

(B) *Fidelity and stability*. As tooth is hard, tooth manipulating in general requests a high stiffness which exceeds the device's maximum stiffness which can be simulated stably. Furthermore, when material is directly removed, discontinuity will be generated on the geometric model of tooth. This will produce discontinuous force feedback and lead to unexpected vibration in the simulation.

By considering these contradictions, we develop a practical approach with high fidelity of feedback force which meanwhile maintains the device in stable. The prototype system by this approach runs with adequate update rates. The main results of our approach are as follows.

(i) To compromise between fidelity and computational efficiency, we derive a simplified tooth grinding force model based on the machining theory and the dynamic behavior of dental handpiece (Section 3).

(ii) To balance between fidelity and stability, we render the force using simulation based method, in contrast to the prevalent direct rendering in previous surgical drilling simulators. The benefit of simulation based method makes it is possible to achieve maximum fidelity while the device maintains stable (Section 4).

(iii) For the implementation of our force model in 3D dental grinding simulation, a layered geometry model is utilized to prevent contact discontinuity caused by direct material removal (Section 5).

2 Related work

There are several haptic enabled surgical drilling simulators developed in various biomedical applications, such as general bone surgery [9], temporal bone surgery [10, 11, 12], craniotomy [13], mastoidectomy [14], orthopedic surgery [15] and dental surgery [1, 2, 3, 4, 5]. They provide various methods for the calculation of feedback force and material removal.

The basic idea for drilling simulation is geometry based. When the tool is penetrated in the bone, response force is calculated from the penetration volume if the tool is represented by a solid object [16, 17], or from penetration depth by simplifying the tool as a point [2, 4]. Meanwhile, the local material is removed as a boolean operation between the tool and the bone geometry. However, immediate removal of the local bone will result in discontinuity between the bone geometries in two consequential time periods, which will cause the discontinuity of penetration volume and depth, and thus lead to unexpected vibration in the simulation. Several works [2, 3] applied a filter using a predefined threshold to smooth the signal before sending it to the device. While this treatment improves the smoothness of the feedback force, the filter can make time delay which may induce instability [18]. Another method to improve the smoothness is the erosion based method proposed by [14]. In contrast to the immediate removal, erosion based method treats the removal as a continuous erosion function of time and applied force. Several parameters need be formulated and tuned, which is not an easy job.

Damping force model for drilling simulation is proposed by Liu [19, 20] based on experimental data of real teeth drilling. A challenge in applying damping force model is that it always leads to instability of the haptic device. This is mainly caused by the fact that the velocity estimation error is derived from position signals. Especially in dental drilling, as the velocity is relatively slow, the velocity error is bigger than the absolute moving velocity which is typically smaller than $0.5mm/s$. Again, filtering method can be applied to smooth the velocity, and it seems stable when the user moves very slowly as demonstrated in our previous work [21]. However, in practical use, the operators always move the handle with a speed exceeding the slow velocity constraint. Then, the filter will lead to large mismatch between the real velocity and the filtered velocity, and leads to unstable results.

A promising but practically difficult approach is physics based drilling force modeling. Unfortunately, the theory of bone drilling is still not clearly explored [22]. The challenge is the complex fracture phenomenon of the bone drilling which differs from the continuous metal drilling. Several pioneers [15, 23] tried to apply metal machining theory in bone drilling simulation. Tsai [15] reported a physics based drilling system for orthopedic surgery. While the force is reported to be similar to the real situation, the material is removed afterwards.

Our method for force computation is stimulated by the physics based force modeling, but differs from those works as we are concerned about the grinding operation with a high stiffness. Besides the machining theory, we also take the behavior of the grinding tool into account. This will be detailed in Section 3.

All above mentioned approaches fall into the direct rendering category. Although this method seems to be very straightforward, it will easily lead to instability as the stiffness of haptic device is limited. In this paper, we explore a simulation based method, known as virtual coupling, to stably render the grinding force. Thus, our approach guarantees maximum fidelity as the coupling spring stiffness is set within the range of the maximally allowed stiffness of a haptic device. Details about the direct and simulation based rendering will be introduced in Section 4.

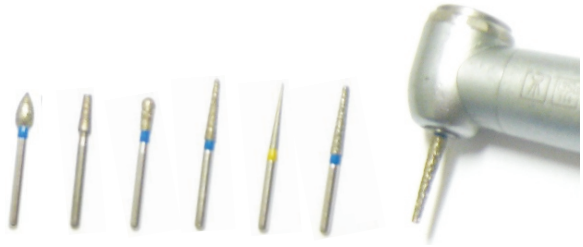

Fig. 2. Burs in different shapes are employed in dental treatments.

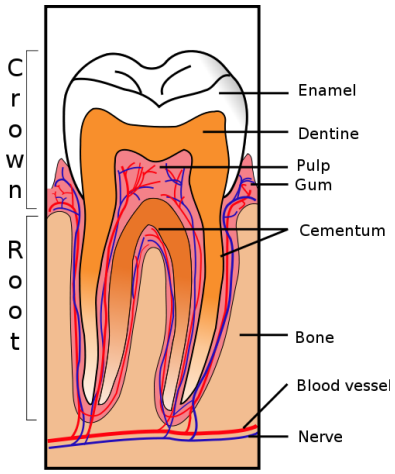

Fig. 3. The illustration of tooth subsections (captured from [24]).

3 Grinding Force Model

The grinding theory of tooth is complex and has not been clearly explored. The feedback force, which is generated by the grinding interaction between the tooth and the dental bur mounted on the handpiece, depends on the behavior of these objects. As both the behavior of the teeth and the dental handpiece (mainly air-turbine handpiece) are different from the metals and tools in metal grinding, the machining theory of metal can not be applied directly. Clinically, the grinding forces are affected by the following factors.

1. *Shape of burs*. As shown in Fig. 2, many different burs could be used in dental treatment. Moreover, the shape of burs will also change after abrasion.
2. *Behavior of handpiece*. Different rotation speeds, forwarding speeds, and powers will also change the value of grinding force significantly.
3. *Behavior of different tooth sections*. A tooth consists of different subsections in different materials (see Fig. 3). When cutting into different sections, different grinding forces will be produced.
4. *Environment*. The environmental factors include the temperature, the cooling water, etc.

By studying the existing grinding theory and the behavior of teeth and handpiece, we are trying to model the haptic sensation features of tooth grinding described by dentists. A simplified model considering only the major factors is developed. More specifically, the handpiece (including its shape, the rotation speed, the forward speed, its stall torque), the contact area and the materials of subsection under processing are major factors affecting the final grinding force. Among these components, the behavior in different subsections, the shape and stall torque of the handpiece is almost constant during the interaction. Other components are interactional during simulation.

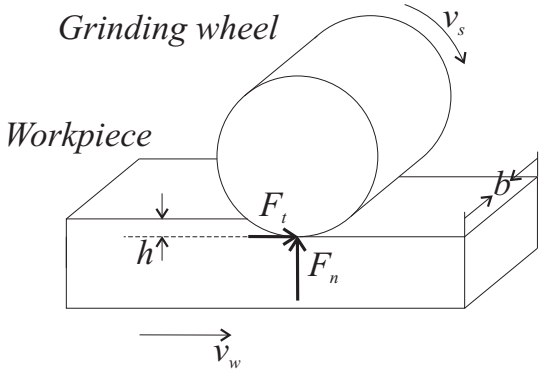

Fig. 4. A typical grinding process. The grinding force is divided into normal grinding force F_n and tangential grinding force F_t.

3.1 Grinding Theory

The grinding theory explains the phenomenon of material removal as a result of the interaction between the cutter and the workpiece. Many researches in bone machining employed the theorem of metal manufacturing in their simulation (e.g., [22]). A typical grinding process is as shown in Fig. 4, where a rotating wheel with linear velocity v_s is grinding on a workpiece with velocity v_w. It should be noted that in dental surgery, the workpiece (tooth) is static, whereas the grinding tool which is held by the dentist approaches the tooth with both rotation and translation velocity. According to the well-established grinding theory introduced in [25], the grinding force can be divided into two parts, the normal grinding force F_n and tangential grinding force F_t. The power of the handpiece is expressed as

$$P = F_t \cdot (v_s \pm v_w) \tag{1}$$

where the plus sign is for up-grinding with the wheel and workpiece velocities v_s and v_w in opposite directions at the grinding zone, and the minus sign is for down-grinding. As v_w is much less than v_s in dental grinding, the power can be further simplified to

$$P = F_t \cdot v_s \tag{2}$$

Chips are formed and removed as a result of the cutting energy. The specific grinding energy, which is defined as the energy required to remove a unit volume of material, can be expressed as

$$u = P/Q_w \tag{3}$$

where Q_w is the volume removed per unit of time. In the configuration as in Fig. 4,

$$Q_w = v_w hb \tag{4}$$

where b and h refer to the grinding width and depth respectively.

The specific grinding energy u is relatively constant in value for a given material and a grinding wheel when there is only small changes in grinding conditions [25]. Thus the tangential force can be approximated as

$$F_t = uQ_w/v_s \tag{5}$$

Meanwhile, we can approximate the normal force since it is in general proportional to the tangential force [25]. We regroup these formulas as

$$\begin{cases} F_t = uv_w hb/v_s \\ F_n = \frac{1}{\alpha} uv_w hb/v_s \end{cases} \tag{6}$$

where α is the coefficient of the relationship between the normal force and tangential force. In this formula, the variables v_w, v_s, h, b can be gotten from the grinding configuration, while the parameters α and u are related to specific material of the workpiece and grinding tool, and can be measured by experiments.

3.2 Force Analysis of Bur

Different from the regular shaped grinding wheels used in manufacturing, the dental bur is rather complex in shape (see Fig. 2). To calculate the overall feedback force in grinding simulation, we have to divide the grinding surface into infinitesimal grinding elements, calculate the force exerted on each small element, and then integrate over the surface to get the final feedback force.

The force analysis of infinitesimal grinding surface is as shown in Fig. 5. The force is divided into the elemental normal force $d\boldsymbol{F}_n$ pointing inwards and the elemental tangential force $d\boldsymbol{F}_t$ along the tangential vector pointing opposite to the rotation direction. By the forces in Eq. 6, we could get

$$\begin{cases} d\boldsymbol{F}_t = u(s)\boldsymbol{v}\cdot\boldsymbol{n}_n(s)\boldsymbol{n}_t(s)\frac{1}{2\pi N r(s)}ds \\ d\boldsymbol{F}_n = \frac{1}{\alpha}u(s)\boldsymbol{v}\cdot\boldsymbol{n}_n(s)(-\boldsymbol{n}_n(s))\frac{1}{2\pi N r(s)}ds \end{cases} \tag{7}$$

where ds is the area of contact element, r is the radius, N is the rotation rate, and $\boldsymbol{n}_n$ and $\boldsymbol{n}_t$ are the normal and tangential vectors. Here, $1/2\pi N r(s)$ is the inverse of rotating velocity v_s in Eq. 6. Since in tooth preparation, patient's tooth is static and the dentist moves the handpiece to grind, the workpiece's velocity v_w is replaced by $\boldsymbol{v}\cdot\boldsymbol{n}_n(s)$, where $\boldsymbol{v}$ is the translational velocity of the handpiece. $\boldsymbol{v}\cdot\boldsymbol{n}_n(s)$ is the velocity projected to the normal direction, thus $\boldsymbol{v}\cdot\boldsymbol{n}_n(s)ds$ is the volume removed per unit of time. Note that we assume the translation velocity at every surface point is the same, which is consistent with the operation principle in tooth preparation. As the same but will be used during the whole procedure of tooth preparation, we assume the parameters $u(s)$ and α are only related to the subsection of tooth under process. We can decide their values by experimental grinding, or tune them on the dentists' evaluation of simulator.

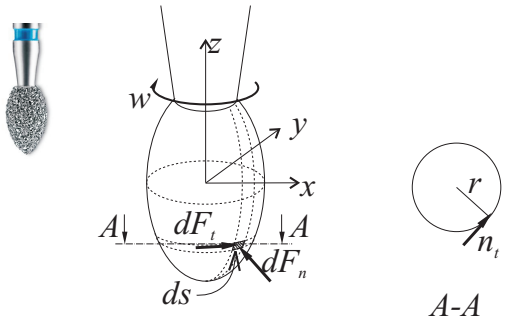

Fig. 5. Force analysis on the surface of bur.

This formula expresses the force acting on a contact element on the surface of the bur. Integrating them, we get the total force $\boldsymbol{F}$ and the total torque T_z around the rotating axis as

$$\boldsymbol{F} = \frac{1}{2\pi N}\iint_D u(s)\boldsymbol{v}\cdot\boldsymbol{n}_n(s)\frac{1}{r(s)}\left[-\frac{1}{\alpha}\boldsymbol{n}_n(s)+\boldsymbol{n}_t(s)\right]ds \tag{8}$$

$$T_z = \iint_D d\boldsymbol{F}_t(s)\boldsymbol{r}(s) = \frac{1}{2\pi N}\iint_D u(s)\,(\boldsymbol{v}\cdot\boldsymbol{n}_n(s))ds \tag{9}$$

where D is the surface of the bur which contacts with the tooth.

3.3 Inspection of Handpiece's Dynamic Behavior

One of the key feature in dental grinding has not been investigated. That is the performance of handpiece when the operator applies too much force during the grinding. In reality, the handpiece will stand still and no materials will be removed from tooth. However, such scenario is dangerous as moving handpiece like that may damage the tooth and even result in handpiece broken. Although experienced dentists would not make this mistake, we still need to inspect this since we are targeting at a simulator for training novices.

The maximum torque of handpiece is expressed as stall torque. It shows a linear relationship with the pressure of the gas, which acts as the power for the handpiece's rotation.

$$\tau_s = \Phi p \tag{10}$$

where p is the gas pressure in bar unit, and Φ is the stall torque coefficient. Typical pressure used in dental grinding is about 2.5 bar, then Φ is found at around 0.4 (ref. [26]).

When the torque is greater than the threshold, the bur will stall then. Thus, we use a Boolean value to indicate the status of the bur.

$$S_{on} = \begin{cases} 1 \text{ if } T_z \le \Phi p \\ 0 \text{ if } T_z > \Phi p \end{cases} \tag{11}$$

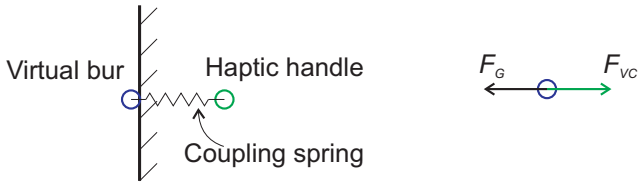

Fig. 6. Virtual coupling scheme: the virtual bur is coupled with the haptic handle through a viscoelastic / elastic spring and the motion of virtual bur is governed by the coupling force and the grinding force.

4 Virtual Coupling based Stable Haptic Rendering

The grinding force model in Eq. 8 indicates that there is a damping effect between the grinding force and the operator's forward velocity. If direct rendering is employed in the display of damping force, the position of haptic device is directly applied to the virtual tool. Collision detection and response are both calculated based on this position, and the resultant force is displayed back directly to the handle of haptic device. However, such direct rendering of damping force is only stable when the damping coefficient is very small – $0.01Ns/mm$ for Phantom is suggested by [19]. However, the damping coefficient in tooth grinding (typically $4Ns/mm$ [19]) is much larger than the threshold of stable direct rendering.

To overcome this difficulty, we conduct an alternative approach, simulation based rendering. In simulation based methods, the position of virtual tool is governed by the coupling force as well as the collision response between the virtual tool and other objects in the virtual environment. In our application of dental grinding, the collision response is the grinding force. A coupling force is defined by adding a virtual viscoelastic / elastic coupling (i.e., a coupling spring [27]) between the positions of the device and the virtual tool. The simulation based method can overcome the small threshold of damping coefficient in direct rendering as stability is now guaranteed by a passive simulation of the virtual tool [28]. By appropriately tuning the parameters of the viscoelastic coupling, stable rendering of large damping coefficient can be obtained.

The virtual coupling in dental grinding is as illustrated in Fig. 6, where the virtual bur is coupled to the haptic handle through a spring. The force exerted on the bur includes the virtual coupling force, $\boldsymbol{F}_{VC}$, computed from Hooke's law and the grinding force, $\boldsymbol{F}_G$, computed from the grinding force model.

$$\boldsymbol{F}_{VC} = k_{VC}(\boldsymbol{P}_{Handle} - \boldsymbol{P}_{Bur}) \tag{12}$$

$$\boldsymbol{F}_G = \boldsymbol{B}_{3\times3}\dot{\boldsymbol{P}}_{Bur} \tag{13}$$

with

$$\boldsymbol{B}_{3\times3} = \frac{1}{2\pi N}\int\!\!\int_D u(s)\frac{1}{r(s)}\left[-\frac{1}{\alpha}\boldsymbol{n}_n(s) + \boldsymbol{n}_t(s)\right]\boldsymbol{n}_n^T(s)ds \tag{14}$$

In these equations, F_{VC} is the virtual coupling force, k_{VC} is the stiffness of the coupling spring, P_{Handle} and P_{Bur} are the position of the haptic handle and the virtual bur respectively, F_G is the grinding force, v shows the forward velocity of the bur, and m is the mass of the bur. k_{VC} is chosen to be smaller than the stiffness of the given haptic device to ensue stability. We denote the state-space of the virtual bur by $\boldsymbol{y}(t) = (\boldsymbol{P}_{Bur}, \boldsymbol{v})^T$, then the translational motion of the virtual bur is governed by the total force as

$$\dot{\boldsymbol{y}}(t) = \begin{pmatrix} \dot{\boldsymbol{P}}_{Bur} \\ \dot{\boldsymbol{v}} \end{pmatrix} = \begin{pmatrix} \boldsymbol{v} \\ (\boldsymbol{F}_{VC} + \boldsymbol{F}_G)/m \end{pmatrix} \tag{15}$$

$\dot{\boldsymbol{y}}(t)$ is expressed as $\boldsymbol{f}(t)$ in the following derivation.

Note that we do not include the rotational coupling in the current setup as in practice the dentists seldom rotate the handpiece when the bur contacts with the tooth. Nevertheless, if needed, the rotation can be easily intergraded in the setup by adding the orientation and angular velocity in the equations of the motion (see [29]).

Applying the explicit Euler's method to solve the haptic rendering problem will induce numerical instability. Therefore, we applied implicit integration method to solve this differential equations, following Baraff's integration method [30]. In the discretized formulation, instead of writing $\boldsymbol{y}_i = \boldsymbol{y}_{i-1} + h\dot{\boldsymbol{y}}_{i-1}$ in Euler's method, we use the backward Euler's formula,

$$\boldsymbol{y}_i = \boldsymbol{y}_{i-1} + h\dot{\boldsymbol{y}}_i \tag{16}$$

where the subscript i refers to the state of current time step, and $i-1$ is the state of previous time step. h is the time step, and $h = 1ms$ is chosen for achieving the $1kHZ$ haptic rendering rate. To solve Eq. 16, we approximate $\dot{\boldsymbol{y}}_i$ by $\dot{\boldsymbol{y}}_{i-1} + \frac{\partial \boldsymbol{f}}{\partial \boldsymbol{y}}\Delta\boldsymbol{y}$ by using the Taylor expression with $\Delta\boldsymbol{y} = \boldsymbol{y}_i - \boldsymbol{y}_{i-1}$. Rearranging these terms, the linear system of equations can be expressed in the form

$$\left(\boldsymbol{I} - h\frac{\partial \boldsymbol{f}}{\partial \boldsymbol{y}}\right)\Delta\boldsymbol{y} = h\boldsymbol{f}_{i-1} \tag{17}$$

where $\boldsymbol{I} - h\frac{\partial \boldsymbol{f}}{\partial \boldsymbol{y}}$ is a 6×6 matrix, and $\frac{\partial \boldsymbol{f}}{\partial \boldsymbol{y}}$ is the Jacobian of the equations of the bur translational motion.

By Eq. 15 and meanwhile taking the assumption that the state of the variables in Eq. 14 are constant during one rendering loop, the Jacobian can be expressed as

$$\frac{\partial \boldsymbol{f}}{\partial \boldsymbol{y}} = \begin{bmatrix} \boldsymbol{0}_{3\times3} & \boldsymbol{I}_{3\times3} \\ -\frac{k_{VC}}{m}I_{3\times3} & \frac{\boldsymbol{B}_{3\times3}}{m} \end{bmatrix} \tag{18}$$

We solve the linear system in Eq. 17 by Gaussian elimination. With the $\Delta\boldsymbol{y}$ obtained from Eq. 17, the current state of the bur and then the corresponding feedback force can be easily computed.

5 Voxel based 3D Grinding

After deriving the formulas about how to compute the forces, we will introduce the implementation details of our

voxel based simulator in this section.

We choose to implement our simulator based on voxel representation for several reasons. Compared with models in mesh representation, voxel-based models [16, 17] provide an intuitive representation for a solid formed by different tissues have different physical properties (e.g., stiffness) in different regions. Moreover, voxel representation is more suitable for material removal simulations such as virtual clay and virtual grinding, where removal can be simply implemented by deleting related voxels. Whereas, complex and time-consuming mesh generation algorithm needs to be developed for such simulations when mesh representation is adopted (e.g., [2]).

An initial system overview of voxel-based simulation has been introduced in our previous publication [21]. In this paper, a new force model is introduced, and a different numerical integration scheme is adopted.

5.1 Material removal

Our method for the material removal is geometry based. Geometrically, two solid bodies such as the tooth and the bur will never occupy a same space in $\Re^3$. Therefore, in the simulation, when the bur contacts the treated tooth, the corresponding voxels in the tooth will be removed. The collision information is detected by checking all voxels of the tool to see if any of them is in the space occupied by voxels of the tooth [21].

The problem with direct removal of collided voxels is that the contact area will change significantly. The maximally allowed displacement $s_{\max}$ of a bur is determined by the maximum velocity of the bur, $v_{\max}$, as

$$s_{\max} = v_{\max}\Delta t \tag{19}$$

with Δt being the time step. In typical dental grinding, the maximum velocity $v_{\max}$ is about $0.5mm/s$. For high fidelity haptic rendering, Δt must be at least $1ms$. Then, we have $s_{max} = 0.0005mm$. Suppose that at a time current t_i, the bur has contacted the tooth, the overlapped voxels are then removed immediately. In the next haptic rendering cycle, the bur's movement must be less than the maximally allowed displacement $s_{\max}$ of the bur. As $s_{max} = 0.0005mm$ is far below the voxel size of the tooth, this means that at the next time current t_{i+1} the bur will lose contact with the tooth. If so, the computed resistance force will be zero as our grinding force model is based on the contact area. When processing material removal in this way, the discontinuity of computed resistance force will occur frequently and will then make the haptic system unstable. This effect can be eliminated by using very high voxel resolution, which however will greatly increase the cost of computational time and memory and is impractical.

To avoid force discontinuity caused by the loss of contact in voxel model, we proposed a two-layer model based material removal method. That is, the voxels of a tooth is removed only when the interior voxels of the bur has overlapped with those tooth voxels. The boundary voxels of a bur are adopted for detecting contact and computing the resistance force, while the interior voxels are used for material removal. After removing the corresponding tooth voxels, the tooth voxels overlapped by the boundary bur voxels will become the new surface of the tooth. Using this method, no matter what size the voxel is, the contact area will not change significantly when removing material (i.e., voxels) from the tooth model. Thus, there is no significant force discontinuity any more. Figure 7 illustrates of our material removal method.

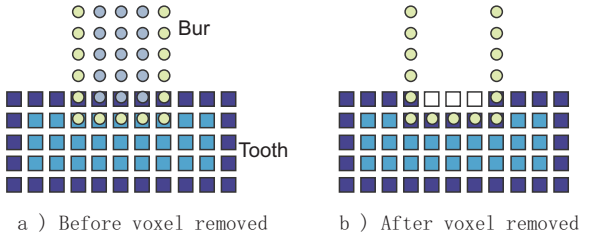

Fig. 7. Material removal: (a) the status at the time current $t = t_i$ and (b) the status at $t = t_{i+1}$ where three voxels in the tooth have been removed. However, the contact area is constant during the material removal. For giving a better illustration, internal voxels of the bur are not displayed in (b).

In practice, as the grinding velocity is relatively low, there is no need for surface updating at every haptic loop. The time span for the interior voxels to contact new surface is about $T = D_{voxel}/v_{max}$ with D_{voxel} being the voxel size and v_{max} being the maximum grinding velocity. Therefore, the appropriate update rate of material removal is

$$f = 1/T = v_{max}/D_{voxel} \tag{20}$$

5.2 Haptic rendering algorithm

The computation flow of haptic rendering is straightforward. In every haptic rendering cycle (1kHZ), we perform the following steps.

1. Update the position and posture of the haptic handle.
2. Check whether the virtual bur and the tooth collide at the previous time step. If not, go back to step 1.
3. Calculate forces at the previous time step: F_G and T_z by Eq. 8 and Eq. 9 respectively, and F_{VC} by Eq. 12.
4. Detect the status of the bur based on Eq. 11 – whether stall or still keep rotating.
5. If the bur stalls, then the position of the virtual bur will not be be updated, and its velocity is assigned to be zero.
6. If the bur still rotates, we calculate the Jacobian based on Eq. 18, and solve Eq. 17 to get the position and velocity change during the last step. Then, the current position and velocity at the current time step can be obtained.
7. Calculate the virtual coupling force of current time step based on Eq. 12, and send the force to haptic device.

In every material removal loop, we check whether there are interval voxels of the handpiece overlapping the voxels of tooth. If yes, remove them. Then, the marching cubes algorithm [31] is employed to generate the mesh surface from the

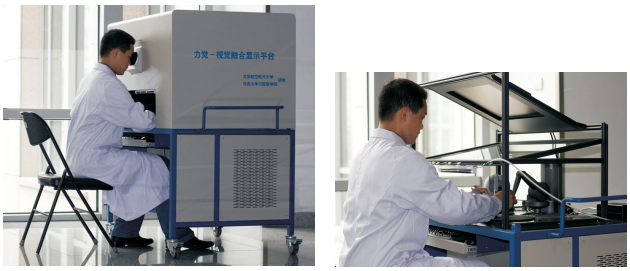

Fig. 8. The left picture shows the training scenario. The internal physical structure of the platform can be found in the right picture, which consists of a computer monitor, two haptic devices, and a half-silvered mirror to co-locate the virtual environment and real hands.

voxels for visual rendering.

6 Experimental Results

The proposed methods have been implemented in Visual Studio 2005 with OpenHaptics and OpenGL, and integrated into a dental training system. This system is composed of two haptic devices (one for dominant operation such as grinding, and the other for auxiliary operation such as using a mouth mirror to assist viewing, see Fig. 1), and a half-silvered mirror to achieve collocated display between the visual and haptic sensation (see Fig. 8). This system is aimed at providing vivid dental training simulation in a college level dentist training course. The haptic device used for grinding operation in our system is the Phantom Desktop from Sensable Technologies, and our computation is conducted on a PC with Intel Core2 Duo CPU and 2GB RAM plus an ATI Radeon X1550 display card with 256MB RAM.

In our experimental tests, the parameters are chosen as follows.

1. *Tooth:* A volume of tooth ($8mm * 8mm * 8mm$) is voxelized with voxel size of $0.1mm$. The specific grinding energy u is assigned with $0.3J/mm^3$ for the hard enamel, and $0.1J/mm^3$ for the soft dentin (see Ref. [32] for the specific cutting energy of bone). The real tooth model is acquired using CT scan with $512 * 512$ resolution where the area occupied by the tooth is around $256 * 256$.
2. *Handpiece and Bur:* A spherical bur (with diameter $1.2mm$) and a cylinder bur (with diameter $1.2mm$ and length $3.0mm$) are also voxelized with the same voxel size as that of the tooth. The coefficient between the tangential force and normal force is chosen as 0.25 [25].

6.1 Evaluation of Force Model

In this experiment, we test the grinding force generated by our method based on the above parameters of tooth, handpiece and bur. Here, we simulate that only one parameter is changed while others retain their initial values.

Material property. Figure 9 shows grinding on the workpiece with different properties when vertically moving a cylinder bur to the surface of a tooth with a constant velocity

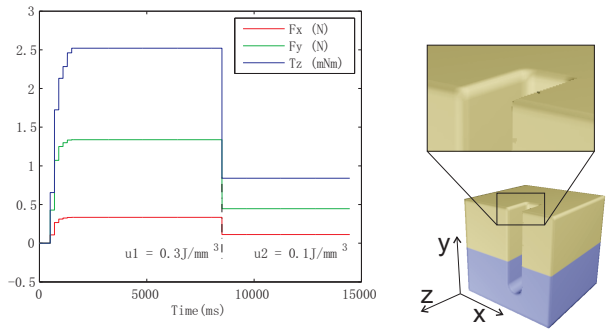

Fig. 9. The specific grinding energy u of the hard enamel is $0.3J/mm^3$ and the energy $0.1J/mm^3$ is for the inner soft dentin. The hard enamel and the soft dentin are shown in different color in the right. The right picture shows the resultant geometry of grinding.

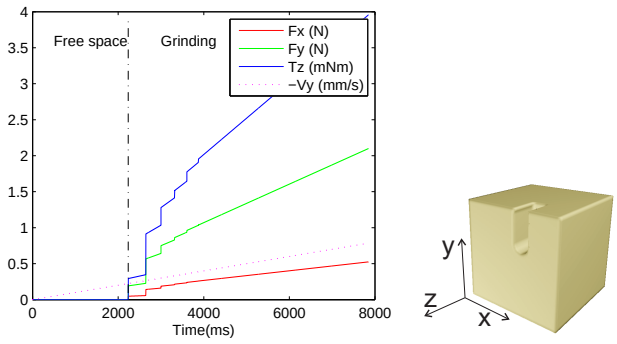

Fig. 10. The magnitude of velocity in y-direction is increasing when vertically moving a cylinder bur to the surface of a tooth. The resultant grinding forces (F_x, F_y) and torque (T_z) are proportional to the change of velocity.

of $0.5mm/s$. At the beginning of the simulation, the bur and the tooth have no collision. From the curves, it is not difficult to find that the grinding force in two directions (F_x, F_y) and the torque (T_z) are proportional to the specific grinding energy of the material, where $u1 = 0.3J/mm^3$ is for the hard enamel (i.e., the first contacted region during grinding) and $u2 = 0.1J/mm^3$ is assigned for the soft dentin.

Grinding velocity. Figure 10 shows the grinding forces generated with variational velocity. Here, when vertically moving a cylinder bur to the surface of a tooth, we increase its velocity with a constant acceleration. From the curve, we find that the grinding forces (F_x, F_y) and the torque (T_z) are proportional to the change of velocity.

Contact area. In this test, when moving the cylinder bur to the surface of tooth, the bur is moved in both y and z directions. Then, the contact area decreases during the procedure of grinding. The resultant grinding force in two directions (F_x, F_y) and the torque (T_z) are as shown in Fig. 11. They are proportional to the contact area.

Different burs. Figure 12 shows the grinding forces generated by moving a ball bur vertically onto the surface of a tooth. It is not difficult to find that the trend of the force and

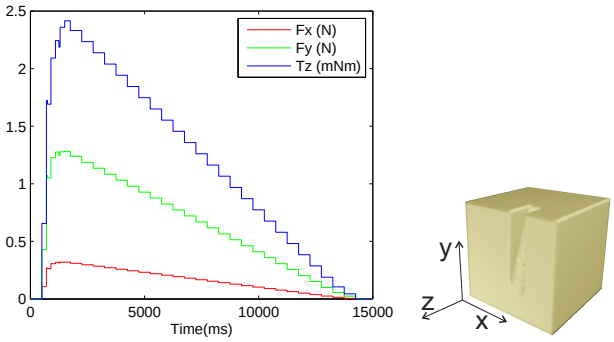

Fig. 11. Grinding with decreased contact area during the simulation. The resultant grinding forces and torque are proportional to the contact area.

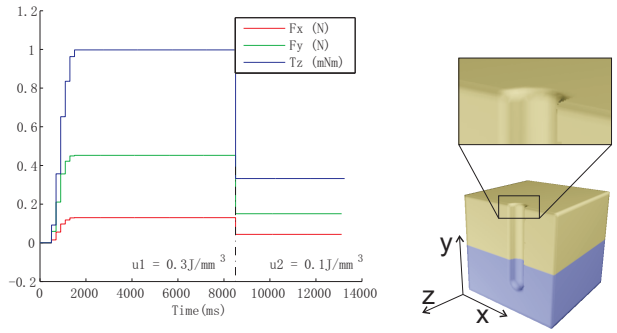

Fig. 12. Grinding using a ball bur. The trend of the forces and torque generated by using a ball bur is similar to that generated by using a cylinder bur (as in Fig. 9). The right picture shows resulting geometry using a ball bur, different from that of using a cylinder bur (as in Fig. 9).

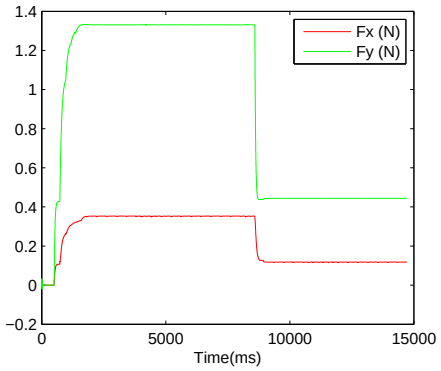

Fig. 13. Virtual coupling based grinding on two different materials. Compared with direct force calculation in Fig. 9, the voxel-effect has been eliminated.

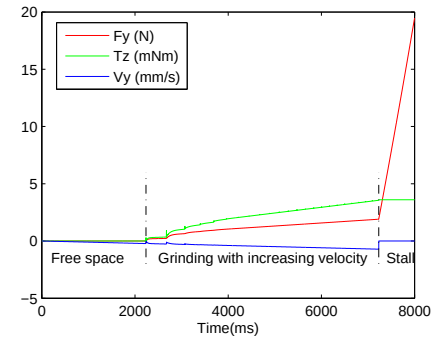

Fig. 14. Grinding with increasing forward velocity. At first, the coupling force and torque is increasing proportional to the value of velocity. When the torque exceeds the stall torque, we will stop moving the virtual bur even if the coupling force increases sharply.

torque using a ball bur is similar to that using a cylinder bur, but the value of resultant forces and torques using a ball bur is smaller. The resultant geometry is different as the head face of the cylinder can produce sharp corner.

Note that although the force curves generated in above tests do not embed vibration with high frequency, we cannot apply these forces directly to the haptic device by using position signals to estimate the velocity. This is because that the position signals usually have sampling errors embedded. Virtual coupling can amend the problem. The artifacts on the force curves are due to the low resolution of voxels – we simply call them voxel-effect in the analysis below.

6.2 Evaluation of Virtual Coupling

In these tests, we calculate the grinding force and the coupling force to derive the position of the virtual bur, and the coupling force is sent to the haptic device.

The time step for integration is same to the haptic update rate (i.e., $1ms$). The mass of the bur is chosen as $8g$. Figure 13 shows the coupling force when grinding on two materials with the same parameters to Fig. 9. Compare these two figures, we can find that the difference between these two forces is small, and the difference can be found at the growing up stage of the force. The coupling force can partly eliminate the voxel effect as it is based on the coupling spring, whose length can not change significantly and thus serves like a filter.

Figure 14 shows the forces when grinding with increasing velocity by using the same parameters as in Fig. 10. Here, in virtual coupling based method, we judge whether the torque is bigger than the stall torque before calculating the new position of the virtual bur. The last section of the Fig. 14 shows that when moving too fast (approximate 0.7mm/s), the torque will be bigger than the stall torque (set as 1.2mNm in our experiment). Then, we will stop moving the virtual bur even if the coupling force is increasing.

We conduct an interactive test to compare the forces generated by the direct rendering versus the virtual coupling. Figure 15 shows the force plot during interaction. The vibration in direct rendering is much larger than that in virtual coupling based approach. In this experiment, the operator tries to move the haptic device with velocity around $0.5mm/s$. However, during the direct rendering, due to the vibration, the operator is sometimes difficult to control the device. The force curve of direct rendering is chosen after

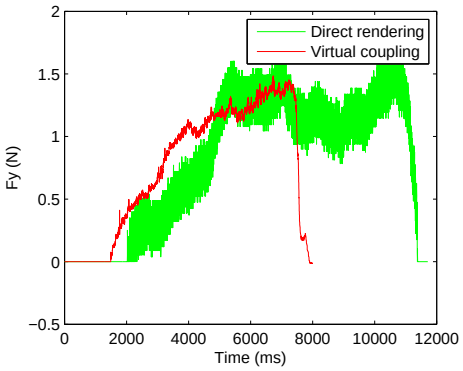

Fig. 15. Forces generated by different approaches – direct rendering vs. virtual coupling based rendering. In the interactive test, the virtual coupling based approach provides more stable feedback force than the direct rendering.

several trials.

The results of designing the tooth cavity and preparing the tooth crown using our system are shown in Fig. 16. The dentist reports that during this operation the force sensation is smooth and feels like grinding on real teeth. Comparing to our previous work in [2], the forces rendered during grinding are more real.

6.3 Discussion

As shown in Figs.9-12, the trends in feedback force with respect to different grinding conditions, material properties, forwarding velocities, contact areas, and different burs are consistent with the haptic sensation in real grinding described by experienced dentists. This validates our simplification on the force model. The feedback force calculated from the grinding force model composed of two components: the force in the forward direction to resist the movement and the resistent force to the rotation. Whereas, our previous works [2,19,21] and other geometry based approaches [4,10] provide only the former one.

Virtual coupling based rendering provides smoother feedback force than the direct rendering (as shown in Fig. 13). However, in the virtual coupling approach, the positions of the virtual bur and the haptic handle are not synchronized. It is similar to the concept of transparency in tele-operation. The displacement between their positions depends on the stiffness of the coupling spring. Further improvement in the hardware will decrease this mismatch and thus improve the fidelity of our simulator.

For haptic enabled simulator in bone machining, while neither the fundamental theory nor the experimental setup is available, one practical way to enhance the fidelity is to communicate more with the experts in the application domain, and try to mimic the subjective sensation by objective simplification of the theory. Specifically designed measurement system will be an important support to evaluate the parameters in the force model, and other approaches, such as measurement based rendering [33], may be also a choice for realistic force calculation.

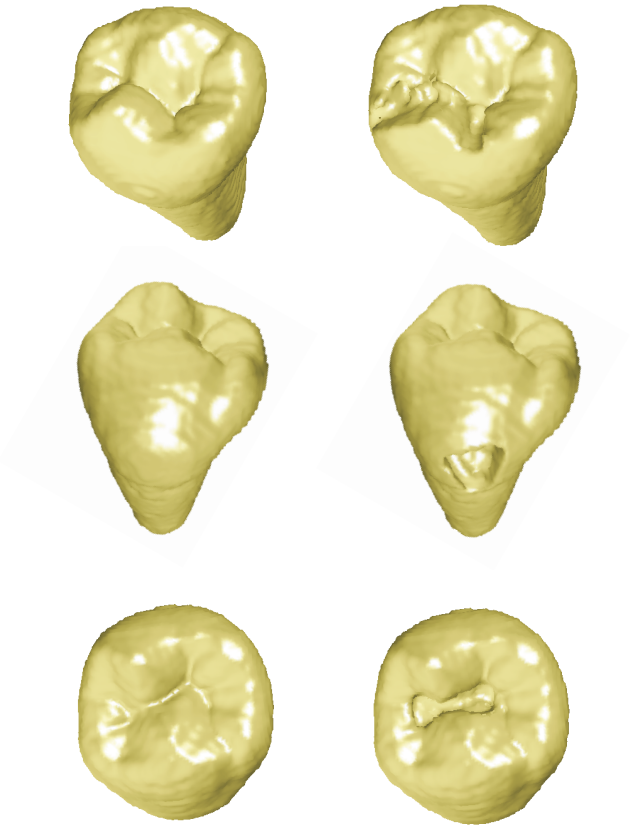

Fig. 16. The results by using our system: left – the original teeth, and right – preparing the crown to mount fake teeth (top row); the prepared class II cavity (middle row); and the prepared class I cavity (bottom row).

To our understanding, the realism has two levels of meaning. Firstly, it refers the trend of the force with respect to different operation conditions. Secondly, on a higher level, the realism should be quantified. Perceptual assessment study is a necessary step for the evaluation a training platform. As there is no useful quantification of realism available currently, we plan to conduct a study with a sufficient number of professional dentists after setting up some quantification criterions with our collaborators in College of Dentistry.

Besides the contact between the bur and the tooth which is investigated in this paper, other kinds of contact may also happen in a virtual training platform, such as the contact between the handle of the handpiece and the tooth, the elastic gums and tongue, and maybe contacts in multiple regions simultaneously. Force modeling of these contacts still needs more effort to make a robust simulator for training purpose.

7 Conclusion

In this paper we present a simplified grinding force model for haptic interaction. The force model is derived from machining theory of grinding by integrating the factors

such the shape of bur and the dynamic behavior of dental handpiece. In our approach, the forces are calculated using virtual coupling to enhance the stability in haptic rendering. Based on these methods, we have developed a voxel-based grinding simulator for tooth preparation training. The results show that the trends in feedback force with respect to different grinding conditions are consistent with the haptic sensation in real grinding described by experienced dentists. Specifically, the force magnitude is different with respect to the forwarding velocity of the bur, the specific energy of the material, the contact area, and different bur shapes. This work also demonstrates that the virtual coupling is effective in eliminating the vibration thus improves the stability of the simulator.

In our current implementation, we target the stability and fidelity. The system can support a virtual environment with 256^3 resolution. As we think, this resolution is not sufficient to represent a whole mouth teeth. Thus, for generating a better simulator in medical training, the memory cost must be minimized and the computational efficiency should be further improved. Possible ways to reach that include to employ some hierarchy data-structure like Octree and to borrow the parallel computational power available on graphics hardware. We consider these as our near future work.

Achnowledgements

This work is supported by the National Science Foundation of China under grant *No*.60605027 and *No*.50575011, the National Hi-tech Research and Development Program of China under grant *No*.2007*AA*01*Z*310, the Hong Kong RGC grant CUHK/417508, and the open project – *Research of GPU-Accelerated Force Rendering on Volumetric Model* – of State Key Lab of Virtual Reality Technology and Systems of China.

References

[1] Chen, L.-Y., Fujimoto, H., Miwa, K., Abe, T., Sumi, A., and Ito, Y., 2003. "A dental training system using virtual reality". In IEEE International Symposium on Computational Intelligence in Robotics and Automation, pp. 430–434.

[2] Wang, D., Zhang, Y., Wang, Y., Lee, Y.-S., Lu, P., and Wang, Y., 2005. "Cutting on triangle mesh: Local model-based haptic display for dental preparation surgery simulation". *IEEE Transactions on Visualization and Computer Graphics,* **11**(6), pp. 671–683.

[3] Yau, H., Tsou, L., and Tsai, M., 2006. "Octree-based virtual dental training system with a haptic device". *Computer-Aided Design & Applications,* **3**(1-4), pp. 415–424.

[4] Kim, L., and Park, S. H., 2006. "Haptic interaction and volume modeling techniques for realistic dental simulation". *The Visual Computer,* **22**(2), pp. 90–98.

[5] Marras, I., Papaleontiou, L., Nikolaidis, N., Lyroudia, K., and Pitas, I., 2006. "Virtual dental patient: a system for virtual teeth drilling". In Multimedia and Expo, IEEE International Conference on, pp. 665–668.

[6] Kolesnikov, M., Zefran, M., Steinberg, A., and Bashook, P., 2009. "Periosim: Haptic virtual reality simulator for sensorimotor skill acquisition in dentistry". In Robotics and Automation, 2009. ICRA '09. IEEE International Conference on, pp. 689–694.

[7] von Sternberg, N., Bartsch, M., Petersik, A., Wiltfang, J., Sibbersen, W., Grindel, T., Tiede, U., Warnke, P., Heiland, M., Russo, P., Terheyden, H., Pohlenz, P., and Springer, I., 2007. "Learning by doing virtually". *International Journal of Oral and Maxillofacial Surgery,* **36**(5), pp. 386–390.

[8] Salisbury, K., Conti, F., and Barbagli, F., 2004. "Haptic rendering: introductory concepts". *Computer Graphics and Applications, IEEE,* **24**(2), pp. 24–32.

[9] Leu, M. C., Niu, Q., and Chi, X. *Virtual Prototyping and Bio Manufacturing*. ch. 2: Virtual Bone Surgery, pp. 21–44.

[10] Pflesser, B., Petersik, A., Tiede, U., Hohne, K. H., and Leuwer, R., 2002. "Volume cutting for virtual petrous bone surgery". *Computer Aided Surgery,* **7**(2), pp. 74–83.

[11] Morris, D., Sewell, C., Barbagli, F., Salisbury, K., Blevins, N. H., and Girod, S., 2006. "Visuohaptic simulation of bone surgery for training and evaluation". *IEEE Comput. Graph. Appl.,* **26**(6), pp. 48–57.

[12] Eriksson, M., Dixon, M., and Wikander, J., 2006. "A haptic vr milling surgery simulator c using high-resolution ct-data". In Medicine Meets Virtual Reality 14, pp. 138–143.

[13] Acosta, E., and Liu, A., 2007. "Real-time volumetric haptic and visual burrhole simulation". In IEEE Virtual Reality Conference, pp. 247–250.

[14] Agus, M., Giachetti, A., Gobbetti, E., Zanetti, G., and Zorcolo, A., 2003. "Real-time haptic and visual simulation of bone dissection". *Presence: Teleoper. Virtual Environ.,* **12**(1), pp. 110–122.

[15] Tsai, M.-D., Hsieh, M.-S., and Tsai, C.-H., 2007. "Bone drilling haptic interaction for orthopedic surgical simulator". *Computers in Biology and Medicine,* **37**(12), pp. 1709–1718.

[16] Avila, R. S., and Sobierajski, L. M., 1996. "A haptic interaction method for volume visualization". In VIS '96: Proceedings of the 7th conference on Visualization, pp. 197–204.

[17] McNeely, W. A., Puterbaugh, K. D., and Troy, J. J., 1999. "Six degree-of-freedom haptic rendering using voxel sampling". In SIGGRAPH '99: Proceedings of the 26th annual conference on Computer graphics and interactive techniques, pp. 401–408.

[18] Colgate, J., and Schenkel, G., 1997. "Passivity of a class of sampled-data systems: application to haptic interfaces". *Journal of Robotic Systems,* **14**(1), pp. 37–47.

[19] Liu, G., Zhang, Y., Wang, D., and Townsend, W. T., 2008. "Stable haptic interaction using a damping model to implement a realistic tooth-cutting simulation for

dental training". *Virtual Reality,* **12**(2), pp. 99–106.

[20] Liu, G., Zhang, Y., and Townsend, W. T., 2008. "Force modelling for tooth preparation in dental training system". *Virtual Reality,* **12**(3), pp. 125–136.

[21] Wu, J., Yu, G., Wang, D., Zhang, Y., and Wang, C. C. L., 2009. "Voxel-based interactive haptic simulation of dental drilling". In ASME IDETC/CIE: International Design Engineering Technical Conferences & Computers and Information in Engineering Conference.

[22] Davidson, S. R. H., and James, D. F., 2003. "Drilling in bone: modeling heat generation and temperature distribution". *ASME Journal of Biomechanical Engineering,* **125**(3), pp. 305–314.

[23] Moghaddam, M., Nahvi, A., Arbabtafti, M., and Mahvash, M., 2008. "A physically realistic voxel-based method for haptic simulation of bone machining". In Proceedings of 6th EuroHaptics Conference, pp. 651–660.

[24] "http://commons.wikimedia.org/wiki/tooth".

[25] Malkin, S., 1989. *Grinding Technology Theory and Applications of Machining with Abrasives*. Society of Manufacturing Engineers.

[26] Dyson, J. E., and Darvell, B. W., 1999. "Torque, power and efficiency characterization of dental air turbine handpieces". *Journal of Dentistry,* **27**(8), pp. 573–586.

[27] Colgate, J., Stanley, M., and Brown, J., 1995. "Issues in the haptic display of tool use". In Proceedings of Intelligent Robots and Systems, IEEE/RSJ International Conference on, Vol. 3, pp. 140–145.

[28] Otaduy, M. A., and Lin, M. C., 2006. *High Fidelity Haptic Rendering (Synthesis Lectures on Computer Graphics and Animation)*. Morgan and Claypool Publishers.

[29] Otaduy, M., and Lin, M., 2005. "Stable and responsive six-degree-of-freedom haptic manipulation using implicit integration". In Proceedings of World Haptics Conference, pp. 247–256.

[30] Baraff, D., and Witkin, A., 1998. "Large steps in cloth simulation". In SIGGRAPH '98: Proceedings of the 25th annual conference on Computer graphics and interactive techniques, pp. 43–54.

[31] Lorensen, W. E., and Cline, H. E., 1987. "Marching cubes: A high resolution 3d surface construction algorithm". *SIGGRAPH Comput. Graph.,* **21**(4), pp. 163–169.

[32] Plaskos, C., Hodgson, A. J., and Cinquin, P., 2003. "Modelling and optimization of bone-cutting forces in orthopaedic surgery". In Medical Image Computing and Computer-Assisted Intervention - MICCAI 2003, pp. 254–261.

[33] Okamura, A. M., Kuchenbecker, K. J., and Mahvash, M., 2008. *Haptic Rendering: Foundations, Algorithms, and Applications*. AK Peters, chap. 21: Measurement-Based Modeling for Haptic Rendering, pp. 443–467.